Wireless Full-Duplex Medium Access Control for Enhancing Energy Efficiency

Makoto Kobayashi, *Student Member, IEEE*, Ryo Murakami, Kazuhiro Kizaki, Shunsuke Saruwatari, *Member, IEEE*, and Takashi Watanabe, *Member, IEEE*

***Abstract*—Recent years have witnessed a proliferation of battery-powered mobile devices, e.g., smartphones, tablets, sensors, and laptops, leading to a significant demand for high capacity wireless communication with high energy efficiency. Among the technologies capable of such efficiency is full-duplex wireless communication, based on the simultaneous uplink and downlink data transmission with limited frequency resources. Previous studies on full-duplex wireless mostly focused on doubling the network capacity, whereas in this paper we discuss how full-duplex wireless can also increase the energy efficiency. We propose low-power communication by wireless full-duplexing (LPFD), taking advantage of the fact that in full-duplex the duration of communication is half that of half-duplex communication. In LPFD, by using the sleep state in which the transceiver in the wireless communication terminal is turned off, the power consumption of the wireless communication terminal is reduced, and the energy efficiency is improved.**

***Index Terms*—Full-duplex, wireless network, energy efficiency, bit-per-Joule.**

I. Introduction

WIRELESS full-duplex communication is becoming a reality with the development of interference cancellation [1]–[7]. Wireless full-duplex communication enables simultaneous transmission and reception in the same frequency band, whereas in current wireless half-duplex communication a transmitter node cannot at the same time receive signals from the other node. This is because a radio wave attenuates strongly over distance, and therefore the signal transmitted by a node would be received by the node itself as being much stronger than the signal received from the other node, thus producing the interference. In contrast, the combination of analog and digital interference cancellation techniques enables the wireless full-duplex communication, and hence doubles the frequency utilization efficiency [1]. Applying wireless full-duplex communication to infrastructure networks [7]–[15] and ad-hoc networks [16]–[19] improves the network throughput.

This paper focuses on the power consumption of wireless full-duplex communication. Low power consumption of wireless full-duplex communication was investigated in [20], where the full-duplex power saving mode (FDPSM) was introduced. This technique reduces the power consumption by turning the media on and off according to a beacon cycle similar to IEEE 802.11 power saving mode (PSM). However, the power consumption of FDPSM is just lower than that of full-duplex communication, but higher than existing half-duplex IEEE 802.11 PSM [21]. Additionally, FDPSM cannot achieve a high throughput because the number of transmissions is limited to one in each beacon cycle.

In this paper, we improve the FDPSM by focusing on the fact that wireless full-duplex communication can reduce the power consumption owing to the combination of uplink and downlink communication at the same time. The occupation time of the full-duplex communication frequency band can be reduced to half that of the wireless half-duplex communication. Additionally, it is possible to share the circuits that consume power by simultaneously performing the uplink and downlink communications. The power consumption model in wireless full-duplex communication is introduced in Section II.

From the perspective of power consumption, we propose low power wireless communication with full-duplexing and control packets (LPFD-PKT) and low power wireless communication with full-duplexing and frequency bitmap (LPFD-FBM). LPFD-PKT reduces the power consumption by scheduling bi-directional full-duplex, two-directional full-duplex, and half-duplex communication using buffer information and inter-user interference information at an access point and at each user terminal. LPFD-FBM reduces the packet exchange overhead of LPFD-PKT by using a frequency bitmap. In addition, scheduling scheme in LPFD-PKT and LPFD-FBM enables user terminals to communicate multiple packets in a beacon cycle.

Several methods for exchanging information by using orthogonal frequency divisional multiplexing (OFDM) subcarriers have been proposed [15], [22]–[26]. The LPFD-FBM uses a frequency bitmap which is an extension of Back2F [22]; this scheme employs subcarriers of OFDM to reduce the random

Manuscript received March 28, 2017; revised July 3, 2017 and September 10, 2017; accepted September 16, 2017. This work was supported in part by the JSPS KAKENHI under Grant JP16H01718, in part by Grant-in-Aid for JSPS Research Fellow under Grant JP17J02859, and in part by the MIC/SCOPE under Grant 155007006. This paper has been presented in part at the IEEE Global Communication Conference Workshop on Full Duplex Wireless Communications, Washington, DC, USA, 2016. The associate editor coordinating the review of this paper and approving it for publication was E. Ayanoglu. *(Makoto Kobayashi and Ryo Murakami are co-first authors.) (Corresponding author: Makoto Kobayashi.)*

The authors are with the Department of Information Networking, Graduate School of Information Science and Technology, Osaka University, Osaka 565-0871, Japan (e-mail: kobayshi.makoto@ist.osaka-u.ac.jp; murakami.ryo@ist.osaka-u.ac.jp; saru@ist.osaka-u.ac.jp; watanabe@ist.osaka-u.ac.jp).

Digital Object Identifier 10.1109/TGCN.2017.2756883

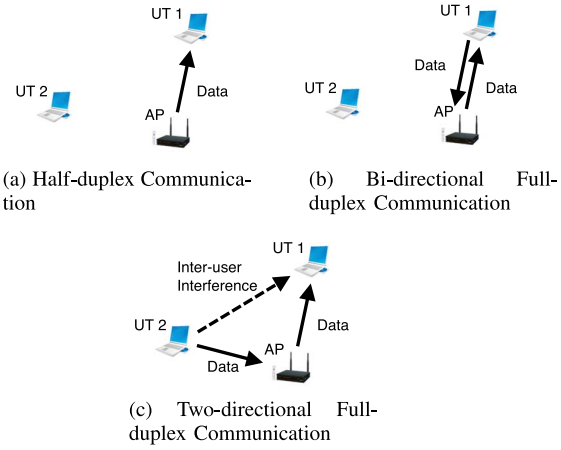

(a) Half-duplex Communication (b) Bi-directional Full-duplex Communication

(c) Two-directional Full-duplex Communication

Fig. 1. Wireless Network.

backoff time by exchanging with other terminals. Because the access point and user terminals in Back2F are assumed to move the transmitting and receiving circuit simultaneously, it is possible to instantaneously exchange the terminal that has the shortest random backoff. Chen *et al.* [15] is the first paper which applies the information exchange by OFDM subcarriers to wireless full-duplexing, and proposes the probabilistic MAC protocol for maximizing the expected network throughput. Back2F and [15] represent the period of random backoff with subcarriers. In contrast, the frequency bitmap in this paper is used for various purposes, such as collection of buffer information, measurement and collection of interference between user terminals, confirmation response, and so on.

The remainder of this paper is organized as follows: Section II introduces the proposed system model; Section III describes LPFD-PKT, which exchanges information via packets; Section IV presents LPFD-FDM, which reduces the information exchange overhead of LPFD-PKT; Section V develops the analytical models of LPFD; Section VI discusses the evaluation of the proposed methods; finally, Section VII shows the discussion and Section VIII concludes the paper.

II. System Model

A. Wireless Full-Duplex

This paper assumes a star topology wireless network consisting of one access point (AP) and N user terminals (UTs) equipped with a wireless full-duplex function. Fig. 1 illustrates the network assumed in this paper. The access point and each user terminal communicate by wireless half-duplex communication (Fig. 1a), wireless bi-directional full-duplex communication (Fig. 1b), and wireless two-directional full-duplex communication (Fig. 1c).

In wireless half-duplex communication, shown in Fig. 1a, the access point transmits one frame to the user terminal, or the user terminal transmits one frame to the access point in a communication period. Wireless half-duplex communication is currently used in normal wireless local area networks (WLANs).

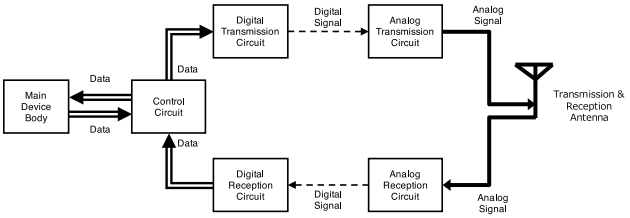

Fig. 2. Model of Half-duplex Communication Circuitss.

In wireless bi-directional full-duplex communication, shown in Fig. 1b, the access point and the user terminal transmit data to each other simultaneously, and both must have a frame for each other.

In wireless two-directional full-duplex communication, shown in Fig. 1c, the access point and two user terminals exchange two frames. One user terminal transmits a frame, and the other user terminal receives a frame. The transmitting user terminal must have a frame for the access point and the access point must have a frame for the receiving user terminal. In wireless two-directional full-duplex communication, an inter-user interference problem occurs when the transmitting user terminal interferes with the receiving user terminal, which then cannot receive the frame from the access point.

B. Transceiver Circuits of Wireless Half-Duplex Communication

Fig. 2 shows a model of the communication circuits of an existing wireless half-duplex communication terminal. Wireless half-duplex transceiver circuits consist of a main device body, a control circuit, a digital transmission circuit, an analog transmission circuit, a digital reception circuit, an analog reception circuit, and a single transmission and reception antenna.

The main device body represents a personal computer or a smartphone that exchanges packets with the control circuit. The control circuit handles the medium access control (MAC) protocol and the ON/OFF switching of the other circuits. The control circuit consumes $P_{\mathrm{CONTROL,ON}}$ [mW] when it is ON, and consumes $P_{\mathrm{CONTROL,OFF}}$ [mW] when it is OFF.

The digital transmission circuit performs the modulation, and the analog transmission circuit converts the digital signal into an analog signal using a digital-to-analog (DA) converter, amplifies the analog signal, and then transmits a radio wave through the antenna. In this paper, the combination of the digital transmission circuit and the analog transmission circuit is designated as the transmission circuit. The transmission circuit consumes $P_{\mathrm{TX,ON}}$ [mW] when it is ON, and consumes $P_{\mathrm{TX,OFF}}$ [mW] when it is OFF.

The analog reception circuit amplifies the received signal, and converts the analog signal into a digital signal with an analog-to-digital (AD) converter. The digital reception circuit then performs the demodulation. In this paper, the combination of the digital reception circuit and analog reception circuit is designated as the reception circuit. The reception circuit consumes $P_{\mathrm{RX,ON}}$ [mW] when it is ON, and consumes $P_{\mathrm{RX,OFF}}$ [mW] when it is OFF.

TABLE I
RELATIONSHIP BETWEEN THE WIRELESS HALF-DUPLEX COMMUNICATION TERMINAL STATE AND CIRCUITS

Communication State	Control Circuit	Transmission Circuits	Reception Circuits
Sleep	OFF	OFF	OFF
Transmission (tx)	ON	ON	OFF
Reception (rx)	ON	OFF	ON

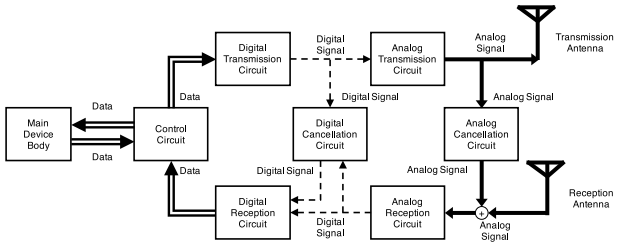

Fig. 3. Model of Full-duplex Communication Circuits.

Table I shows the relationship between the states of wireless half-duplex communication terminal and circuits. In the power consumption model, the control circuit, the transmission circuit, and the reception circuit are OFF when the wireless half-duplex communication terminal is in sleep state; the control circuit and transmission circuit are ON when the terminal transmits data; the control circuit and the reception circuit are ON when the terminal receives data.

We can derive the power consumption of the whole transceiver circuits from the relationship between the states of the wireless half-duplex communication terminal and circuits. The power consumption of the whole transceiver circuits for each state $(f_{\mathrm{HD}}(s)|s \in \{\text{sleep, tx, rx}\})$ is given by:

$$\begin{aligned} f_{\mathrm{HD}}(\text{sleep}) &= P_{\mathrm{CONTROL,OFF}} + P_{\mathrm{TX,OFF}} + P_{\mathrm{RX,OFF}} \\ f_{\mathrm{HD}}(\text{tx}) &= P_{\mathrm{CONTROL,ON}} + P_{\mathrm{TX,ON}} + P_{\mathrm{RX,OFF}} \\ f_{\mathrm{HD}}(\text{rx}) &= P_{\mathrm{CONTROL,ON}} + P_{\mathrm{TX,OFF}} + P_{\mathrm{RX,ON}}. \end{aligned}$$

C. Transceiver Circuits of Wireless Full-Duplex Communication

Fig. 3 shows a model of the communication circuits of a wireless full-duplex communication terminal. It includes digital and analog cancellation circuits, not present in the half-duplex communication terminals, that have the purpose of canceling the self-interference. In this paper, the combination of the digital and analog cancellation circuits is designated as the cancellation circuit, and consumes $P_{\mathrm{CANCEL,ON}}$ [mW] when it is ON, and consume $P_{\mathrm{CANCEL,OFF}}$ [mW] when it is OFF.

Fig. 3 shows an example of a full-duplex communication terminal, which has two antennas for transmission and reception, respectively. However, there also exists full-duplex communication terminals having only one antenna. For example, in [1], the transmission and reception circuits share a single antenna by using a circulator for full-duplex communication.

Table II shows the relationship between the states of the wireless full-duplex communication terminal and circuits. The difference from the half-duplex communication is that a cancellation circuit is added to the system and a full-duplex communication state is added to the states. The cancellation circuit is ON only when the terminal is in the full-duplex communication state. In this state, all the terminal circuits are also ON, i.e., the control circuit, the transmission and reception circuits, and the cancellation circuit.

TABLE II
RELATIONSHIP BETWEEN THE STATE OF THE WIRELESS FULL-DUPLEX COMMUNICATION TERMINAL AND CIRCUITS

Communication State	Control Circuit	Transmission Circuits	Reception Circuits	Cancel Circuits
Sleep	OFF	OFF	OFF	OFF
Transmission (tx)	ON	ON	OFF	OFF
Reception (rx)	ON	OFF	ON	OFF
Full-duplex (fd)	ON	ON	ON	ON

We can derive the power consumption of the whole transceiver circuits from the relationship between the states of the wireless full-duplex communication terminal and circuits. The power consumption of the whole transceiver circuits in each state $(f_{\mathrm{FD}}(s)|s \in \{\text{sleep, tx, rx, fd}\})$ is given by:

$$\begin{aligned} f_{\mathrm{FD}}(\text{sleep}) &= P_{\mathrm{CONTROL,OFF}} + P_{\mathrm{TX,OFF}} + P_{\mathrm{RX,OFF}} + P_{\mathrm{CANCEL,OFF}} \\ f_{\mathrm{FD}}(\text{tx}) &= P_{\mathrm{CONTROL,ON}} + P_{\mathrm{TX,ON}} + P_{\mathrm{RX,OFF}} + P_{\mathrm{CANCEL,OFF}} \\ f_{\mathrm{FD}}(\text{rx}) &= P_{\mathrm{CONTROL,ON}} + P_{\mathrm{TX,OFF}} + P_{\mathrm{RX,ON}} + P_{\mathrm{CANCEL,OFF}} \\ f_{\mathrm{FD}}(\text{fd}) &= P_{\mathrm{CONTROL,ON}} + P_{\mathrm{TX,ON}} + P_{\mathrm{RX,ON}} + P_{\mathrm{CANCEL,ON}}. \end{aligned}$$

D. Bit-Per-Joule

This paper uses bit-per-Joule (BPJ) [bits/J] as an index of energy consumption efficiency in frame transmission and reception. BPJ is the amount of data transmitted per unit energy consumption. The higher the BPJ, the larger the amount of data that can be transmitted with the same energy consumption. The value of BPJ is the same as the bits per second per Watt [bps/W].

In the model of the wireless full-duplex communication shown in Section II-C, the average power consumption of terminals is $\bar{P} = \frac{\sum_{s\in S} f_{\mathrm{FD}}(s) t_s}{\sum_{s\in S} t_s}$, where $S(= \{\text{sleep, tx, rx, fd}\})$ denotes all states, and t_s represents the time spent in the state s. The average throughput is $\bar{R} = \frac{C t_{\mathrm{tx}} + C t_{\mathrm{rx}} + 2 C t_{\mathrm{fd}}}{\sum_{s\in S} t_s} = \frac{C(t_{\mathrm{tx}} + t_{\mathrm{rx}} + 2 t_{\mathrm{fd}})}{\sum_{s\in S} t_s}$. Thus, we can express the value of BPJ [bits/J] as,

$$\mathrm{BPJ} = \frac{\bar{R}}{\bar{P}} = \frac{C(t_{\mathrm{tx}} + t_{\mathrm{rx}} + 2t_{\mathrm{fd}})}{\sum_{s\in S} f_{\mathrm{FD}}(s) t_s}.$$

III. LOW POWER WIRELESS COMMUNICATION WITH FULL-DUPLEXING AND CONTROL PACKETS

Based on the power model of Section II, we design a low power wireless communication with full-duplexing and control packets (LPFD-PKT) that realizes low power wireless communication using wireless full-duplex communication. In LPFD-PKT, the access point assigns each frame to bi-directional full-duplex, two-directional full-duplex, or half-duplex communication. The access point uses information about the buffered packets in the access point and user terminals, and inter-user interference to assign the communication schedule.

A. Energy Efficiency of Communication Method

The LPFD-PKT design focuses on the fact that bi-directional full-duplex communication achieves the highest energy efficiency of all communication methods, i.e., bi-directional full-duplex, two-directional full-duplex, and half-duplex communication. $\mathrm{BPJ}_{\mathrm{BFD}}$, $\mathrm{BPJ}_{\mathrm{TFD}}$, and $\mathrm{BPJ}_{\mathrm{HD}}$ are defined as the BPJ of bi-directional full-duplex, two-directional full-duplex, and half-duplex communication, respectively. In this section, we assume symmetric traffic that both of the access point and a user terminal have $C\tau$ [bits] data to transmit at some point in time for simplicity. Note that asymmetric traffic will be considered in the simulation of Section VI-G.

First, in bi-directional full-duplex communication, the access point and user terminal transmit $C\tau$ [bits] data, respectively, in the same time duration τ. During τ, the user terminal consumes the power corresponding to full-duplex communication, and its BPJ is given by:

$$\begin{aligned}\mathrm{BPJ}_{\mathrm{BFD}} &= \frac{2\times C\tau}{f_{\mathrm{FD}}(\mathrm{fd})\tau} \\ &= \frac{2C}{P_{\mathrm{CONTROL,\,ON}} + P_{\mathrm{TX,\,ON}} + P_{\mathrm{RX,\,ON}} + P_{\mathrm{CANCEL,\,ON}}}.\end{aligned} \tag{1}$$

In two-directional full-duplex communication, the access point and user terminal transmit $C\tau$ [bits] data, respectively, in the same time duration τ. Note that two user terminals participate in two-directional full-duplex communication. During the transmission duration τ, one user terminal consumes power for transmission and the other consumes power for reception. The BPJ of two-directional full-duplex communication is

$$\begin{aligned}\mathrm{BPJ}_{\mathrm{TFD}} &= \frac{C\tau + C\tau}{f_{\mathrm{FD}}(\mathrm{tx})\tau + f_{\mathrm{FD}}(\mathrm{rx})\tau} \\ &= \frac{2C}{2P_{\mathrm{CONTROL,\,ON}} + P_{\mathrm{TX,\,ON}} + P_{\mathrm{RX,\,ON}}}.\end{aligned} \tag{2}$$

In half-duplex communication, the access point and user terminal transmit $C\tau$ [bits] data each in time division. The duration of half-duplex communication becomes therefore 2τ. The user terminal consumes power for transmission and reception in the respective duration τ. The BPJ of half-duplex communication is

$$\begin{aligned}\mathrm{BPJ}_{\mathrm{HD}} &= \frac{C\times 2\tau}{f_{\mathrm{FD}}(\mathrm{tx})\tau + f_{\mathrm{FD}}(\mathrm{rx})\tau} \\ &= \frac{2C}{2P_{\mathrm{CONTROL,\,ON}} + P_{\mathrm{TX,\,ON}} + P_{\mathrm{RX,\,ON}}}.\end{aligned} \tag{3}$$

By combining (2) and (3), we find $\mathrm{BPJ}_{\mathrm{TFD}} = \mathrm{BPJ}_{\mathrm{HD}}$. Additionally, we can assume $P_{\mathrm{CONTROL,\,ON}} > P_{\mathrm{CANCEL,\,ON}}$ in general. By combining (1) and (2), and assuming $P_{\mathrm{CONTROL,\,ON}} > P_{\mathrm{CANCEL,\,ON}}$, we obtain

$$\mathrm{BPJ}_{\mathrm{BFD}} > \mathrm{BPJ}_{\mathrm{TFD}} = \mathrm{BPJ}_{\mathrm{HD}}.$$

B. Operation of LPFD-PKT

LPFD-PKT comprises 4 phases as follows:

1) Beacon frame exchange phase
2) Buffered packet notification and inter-user interference measurement phase
3) Transmission schedule assignment phase
4) Data transmission and acknowledgment phase.

Each user terminal exchanges authentication information when connecting to the access point, and, at the same time, receives the number of user terminals connected to the access point (N) and the node ID (Node-ID). Node-ID is an integer number from 0 to N and is used for uniquely identifying the access point and user terminal in the network. Node-ID 0 denotes the access point.

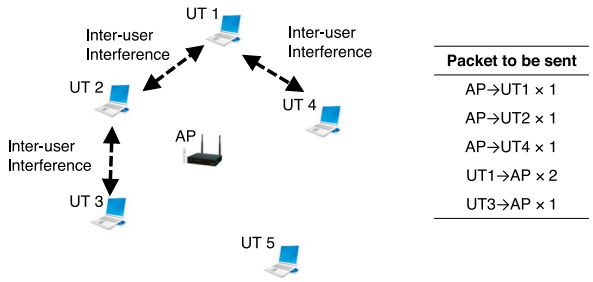

Fig. 4. Wireless Network: One Access Point and 5 User Terminals.

Fig. 4 shows an example of wireless network consists of one access point and five user terminals. In Fig. 4, inter-user interference is present between user terminals 1 and 2, between user terminals 1 and 4, and between user terminals 2 and 3. Fig. 5 shows an example of the frame sequence of the LPFD-PKT for the topology of Fig. 4. In Fig. 4 and Fig. 5, we assume that the access point has a packet to user terminal 1, a packet to user terminal 2, and a packet to user terminal 4; user terminal 1 has two packets to send to the access point; user terminal 3 has a packet to send to the access point when the beacon frame is exchanged.

The "beacon frame exchange phase" occurs periodically every t_{beacon}, where t_{beacon} is the beacon interval length. The access point periodically transmits the beacon frame, indicating the number of user terminals connected to the access point (N). User terminals that receive a beacon frame synchronize their clocks with the access point. In the "buffered packet notification and inter-user interference measurement phase," each user terminal transmits a buffer information (BI) frame and sends the number of buffered packets to the access point. At the same time, user terminals measure the inter-user interference. Details regarding the "buffered packet notification and inter-user interference measurement phase" are described in Section III-C. In the "transmission schedule assignment phase," the access point assigns each frame to bi-directional full-duplex, two-directional full-duplex, and half-duplex communication, relying on a user interference information request (UIR) frame and a user interference information (UII) frame. More details regarding the "transmission schedule assignment phase" are described in Section III-D. In the "data transmission and acknowledgment phase," the access point informs the schedule of transmission by sending the schedule (SCHED) frame that will be followed by the user terminals to transmit and receive data frames.

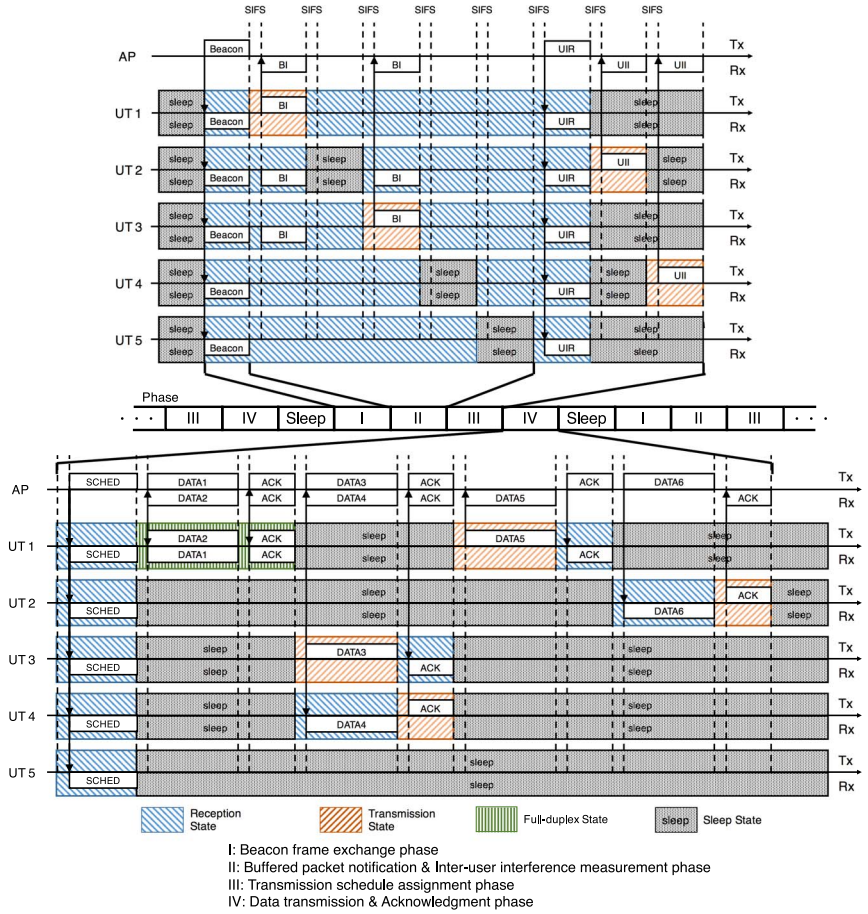

Fig. 5. Low Power Wireless Communication with Full-duplexing and Control Packets (LPFD-PKT).

Upon reception, the access point and user terminals exchange an acknowledgment (ACK) frame. Further details on the "data transmission and acknowledgment phase" are described in Section III-E.

The proposed LPFD-PKT and LPFD-FBM can be made compatible with existing carrier sense multiple access with collision avoidance (CSMA/CA) compliant half-duplex devices by using the same mechanism as the existing IEEE 802.11 PSM. In the proposed method and IEEE 802.11 PSM, the access point acquires a carrier with a beacon frame by using CSMA/CA mechanism and updates network allocation vector (NAV) of other nodes with sequential control frames. The way that the access point acquires a carrier with the beacon frame can coexist with the half-duplex user terminal operating with CSMA/CA.

C. Buffered Packet Notification and Inter-User Interference Measurement Phase

User terminals send notification of their buffered packets and measure inter-user interference to obtain information to be used in the transmission schedule assignment phase, described in Section III-D. Because bi-directional full-duplex communication can enhance the energy efficiency of user terminals, the access point schedules a transmission to create bi-directional full-duplex communication by obtaining the buffered packet in user terminals. Additionally, the access point schedules two-directional full-duplex communication to avoid inter-user interference by gathering information regarding inter-user interference. Inter-user interference would waste the power consumed by the user terminal for downlink reception during two-directional full-duplex.

Each user terminal switches from sleep state to awake state at every beacon interval, receives the beacon frame from the access point, and transmits the BI frame in the order assigned to the Node-ID after reception of the beacon frame. The BI frame includes the Node-ID of the BI frame source and number of data frames held by the user terminal in the buffer. In the example of Fig. 5, it is assumed that user terminal 1 notifies that it has two frames for the access point, and user terminal 3 notifies that it has one frame for the access point, respectively. Instead, user terminals 2, 4, and 5 switch to sleep state during the duration of their BI frame transmission because they do not have buffered data for the access point.

All user terminals remain in awake state for the duration of the BI frame transmission from other user terminals in order to receive the BI frame from them. In the example shown in Fig. 5, user terminal 2 receives BI frames from user terminals 1 and 3, and determines that inter-user interference has occurred

Algorithm 1: LPFD Transmission Scheduling

```
   Input: U, D
1  // Arrays of uplink and downlink packets to send
   Output: Q
2  // Communication Schedule Array
3  Q ← ∅, Q_BFD ← ∅, Q_TFD ← ∅, Q_HD ← ∅
4  foreach u ∈ U do
5      foreach d ∈ D do
6          if u.src is equal to d.dst then
7              push (u, d) to Q_BFD
8              // Assign bi-directional full-duplex
                  communication
9              U ← U\u, D ← D\d
10 if D ≠ φ then
11     Request inter-user interference information to d.dst
       s.t. d ∈ D
12     Records inter-user interference information.
13 foreach u ∈ U do
14     foreach d ∈ D do
15         if Transmission of the uplink packet "u" dose not
           interfere "d.dst" then
16             push (u, d) to Q_TFD
17             // Assign two-directional full-duplex
                  communication
18             U ← U\u, D ← D\d
19     push (u, φ) to Q_HD
20     // Assign uplink half-duplex communication
21     U ← U\u
22 foreach d ∈ D do
23     push (φ, d) to Q_HD
24     // Assign downlink half-duplex communication
25     D ← D\d
26 Q ← Q_BFD + Q_TFD + Q_HD
27 return
```

between itself and user terminals 1 and 3. User terminal 4 determines that inter-user interference occurred between itself and user terminal 1, because it received the BI frame from user terminal 1. User terminals 1, 3, and 5 determine that they were not influenced by any inter-user interference because they did not receive a BI frame.

D. Transmission Schedule Assignment Phase

In the "transmission schedule assignment phase," the access point schedules the transmission using the received BI frames. In order to enhance the energy efficiency and maintain a high throughput, the access point assigns the transmission in this order:

1) bi-directional full-duplex communication
2) two-directional full-duplex communication
3) half-duplex communication.

Algorithm 1 shows the proposed transmission scheduling algorithm, whose variables are as follows. The variable U represents an array of uplink packets to send, and the variable D represents an array of downlink packets to send. The variables U and D store packets in the order of Node-ID. The variable $u\,(\in U)$ represents an uplink packet to send; and the variable $d\,(\in D)$ represents a downlink packet to send. The variable $u.src$ is the Node-ID of the source user terminal of the uplink packet (u). The variable $d.dst$ is the Node-ID of the destination user terminal of the downlink packet (d). The variable Q is the assigned transmission schedule.

Details of the transmission scheduling are described as follows. First, the access point assigns the bi-directional full-duplex in lines 4–9 of Algorithm 1. If downlink packets remain, the access point requests their destination user terminals to send the inter-interference information in lines 10–12. Second, the access point schedules the two-directional full-duplex in lines 15–18, based on the inter-user interference information. Third, the access point assigns the uplink half-duplex communication in lines 19–21. Finally, the access point allocates the downlink half-duplex communication in lines 23–25.

The access point allocates the transmission order by using the Node-ID. Each node has a Node-ID which is assigned by the access point when the user terminal associates with the network. The access point allocates the communication following the order of the user terminal with lowest Node-ID for each communication types, i.e., bi-directional full-duplex, two-directional full-duplex, half-duplex communication.

In the example of Fig. 5, the access point first assigns the bi-directional communication and detects the uplink and downlink pair. The access point has a data frame for the user terminal 1, and the user terminal 1 has two data frames for the access point. Thus, the access point assigns bi-directional full-duplex communication between the access point and user terminal 1 for the first cycle.

Second, the access point assigns two-directional full-duplex communication. The access point collects information regarding inter-user interference via UIR and UII frames in order to determine the uplink and downlink combinations of two-directional full-duplex communication. The UIR frame contains the Node-IDs of user terminals that are expected to participate in two-directional full-duplex communication. Node-IDs in the UIR frame are arranged in the order of UII frame transmission. A user terminal whose Node-ID is included in the UIR frame returns the UII frame to the access point according to the Node-ID order in the UII frame. The UII frame includes the Node-IDs of all user terminals where inter-user interference occurs with the terminal that transmitted the UII frame. Inter-user interference is measured by the BI frame mentioned in Section III-C.

In the example of Fig. 5, user terminals 2 and 4 are candidates for two-directional full-duplex communication receiver, and the access point requests them to transmit the UII frame by sending the UIR frame. User terminals 2 and 4 transmit the UII frame after receiving the UIR frame. User terminal 2 notifies the access point that inter-user interference occurred with user terminals 1 and 3, and user terminal 3 notifies the access point that inter-user interference occurred with user terminal 1.

The access point determines the uplink and downlink combination of two-directional full-duplex communication based on the inter-user interference information. At that time, the access point generates the uplink and downlink combination of two-directional full-duplex communication, such that inter-user interference does not occur. In this example, the access point knows that user terminal 1 and 3 both have one remaining data frame to transmit after bi-directional full-duplex communication. Additionally, the access point buffers one data frame for user terminal 2 and another frame for user terminal 4. The access point assigns a two-directional full-duplex communication (uplink source is user terminal 3; and downlink destination is user terminal 4) to the second transmission cycle.

Finally, the access point schedules half-duplex communication, where the remaining data frames not subject to bi-directional or two-directional full-duplex communication are transmitted. In the example shown in Fig. 5, during the third transmission cycle, user terminal 1 transmits a data frame to the access point; and during the fourth transmission cycle, the access point transmits data to user terminal 2.

E. Data Transmission and Acknowledgment Phase

In the data transmission and acknowledgment phase, all user terminals first switch from sleep state to awake state in order to receive the SCHED frame from the access point. The access point transmits the SCHED frame and notifies all user terminals of the data frame transmission order. The SCHED frame contains information regarding the cycle in which each user terminal will transmit the uplink and downlink. The access point and the user terminals transmit and receive the data frame and the ACK frame according to the schedule described in the SCHED frame. User terminal switches back to sleep state when it does not transmit or receive data, or ACK frames, in order to reduce the energy consumption.

In the example shown in Fig. 5, the first cycle of communication is bi-directional full-duplex communication between the access point and user terminal 1. The second communication cycle is two-directional full-duplex communication in which user terminal 3 transmits data to the access point and the access point transmits data to user terminal 4. In the third communication cycle, half-duplex communication from user terminal 1 is performed. Finally, in the fourth communication cycle, half-duplex communication to user terminal 2 is performed.

IV. Low Power Wireless Communication With Full-Duplexing and Frequency Bitmap

In the LPFD-PKT described in Section III, the gathering of information on buffered packets, inter-user interference, and ACK frames, becomes an overhead. Particularly, the number of frames for gathering the inter-user interference information increases exponentially with the number of user terminals. Low power wireless communication with full-duplexing and frequency bitmap (LPFD-FBM) has also four phases as the LPFD-PKT, e.g., beacon frame exchange phase, buffered packet notification and inter-user interference measurement phase, transmission schedule assignment phase, data transmission and acknowledgment phase. However, in contrast to LPFD-PKT, LPFD-FBM reduces the overhead by using a combination of full-duplex communication and frequency bitmap. Specifically, LPFD-FBM uses 5 types of frequency bitmap, namely: buffer information frequency bitmap (BI-FBM) that reduces the overhead of gathering the buffered packet information; user interference information request frequency bitmap (UIR-FBM) and user interference information frequency bitmap (UII-FBM) that reduce the overhead of gathering the inter-user interference information; schedule frequency bitmap (SCHED-FBM) that reduces the overhead of the transmission schedule notification by the access point to user terminals; and acknowledgment frequency bitmap (ACK-FBM), to reduce the acknowledgment overhead.

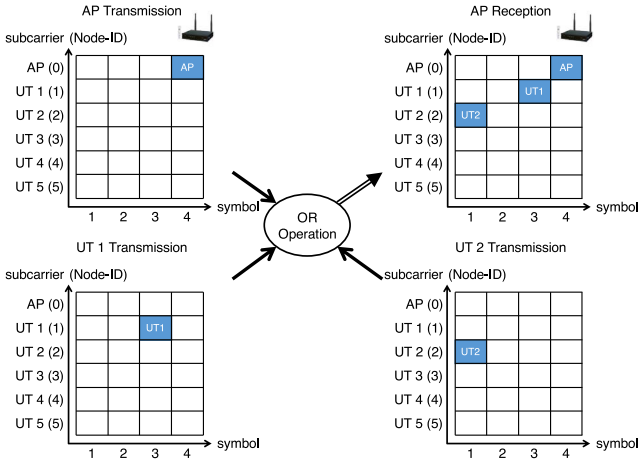

Fig. 6. Frequency Bitmap.

A. Frequency Bitmap

A frequency bitmap is a technology that allows multiple terminals to simultaneously and bi-directionally transmit information by combining the presence and absence of OFDM signal subcarriers and wireless full-duplex communication. Fig. 6 shows an example of a frequency bitmap. The frequency bitmap has a frequency domain part and a time domain part. The frequency domain part of the frequency bitmap is divided by the OFDM signal subcarriers. The time domain part is divided by the OFDM symbols. One subcarrier in one OFDM symbol is represented by one bit. Each user terminal receives the Node-ID, which is assigned to the user terminal when the user terminal associates with the network.

A user terminal or the access point receives duplicated frequency bitmap signals when multiple nodes transmit a frequency bitmap simultaneously. This duplication is similar to an OR operation. By using the frequency bitmap characteristics, the access point and the user terminals can receive information from many nodes simultaneously. Additionally, wireless full-duplex communication enables simultaneous transmission and reception, allowing many nodes to exchange information simultaneously and bi-directionally.

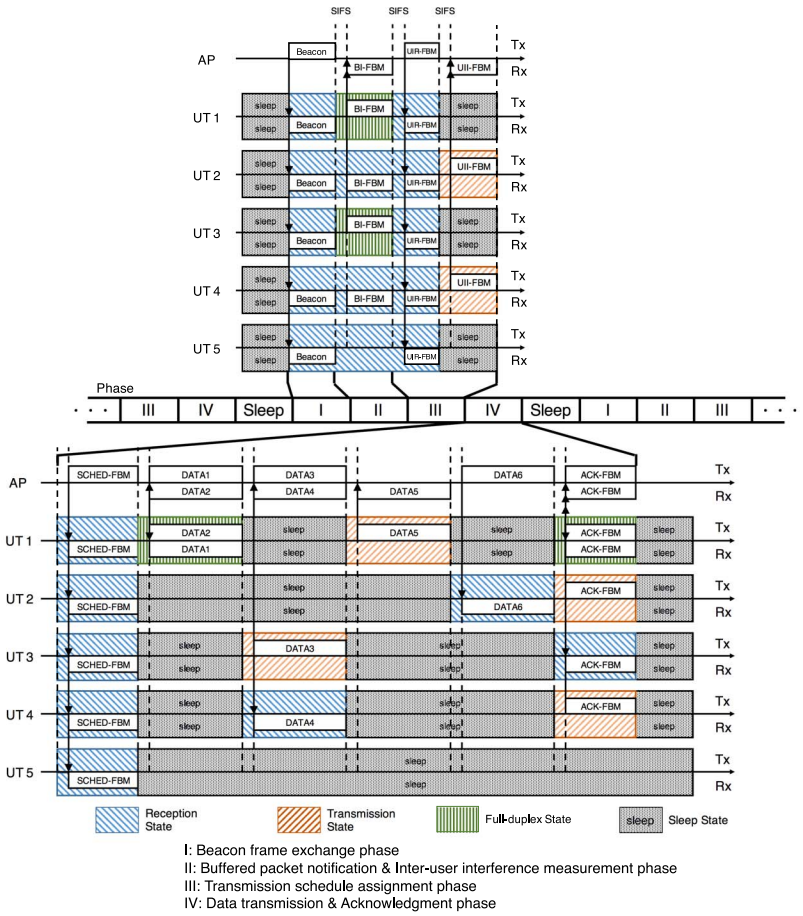

Fig. 7. Low Power Wireless Communication with Full-duplexing and Frequency Bitmap (LPFD-FBM).

Fig. 7 illustrates an example of an LPFD-FBM time sequence in a topology composed of one access point and five user terminals, as shown in Fig. 4. In the example of Fig. 7, it is assumed that the access point has a data frame for user terminals 1, 2 and 4, user terminal 1 has two data frames for the access point, and user terminal 3 has a data frame at the moment of the beacon frame exchange. All user terminals switch from sleep state to awake state to receive the beacon frame at every beacon interval. LPFD-FBM uses the same beacon frame as the LPFD-PKT frame, mentioned in Section III.

All user terminals that receive the beacon frame, send a notification of buffered packets in each user terminal using BI-FBM. Moreover, all user terminals measure at the same time the inter-user interference by receiving the BI-FBM from other user terminals with full-duplex reception circuits. Details of the BI-FBM will be mentioned in Section IV-B.

The access point schedules bi-directional full-duplex communication after receiving BI-FBMs. Then, the access point informs the reception destination candidates of downlink two-directional full-duplex communication by transmitting a UIR-FBM to all user terminals. User terminals that are listed as candidates, transmit the UII-FBM that indicates the inter-user interference of the transmitting user terminal. More details regarding the UIR-FBM and UII-FBM are given in Sections IV-C and IV-D, respectively.

After receiving the UII-FBM frames, the access point schedules the data frame transmission by using buffered packets in the access point and all user terminals, and inter-user interference information. The scheduling algorithm uses the same procedure as LPFD-PKT. The access point transmits to all user terminals the SCHED-FBM that contains the transmission schedule information. More details regarding SCHED-FBM are given in Section IV-E.

The user terminal that receives the SCHED-FBM transmits and receives the data frames according to the schedule predetermined by the access point. When the transmission and reception of all data frames have been completed, the access point and all user terminals exchange the ACK-FBM, which acknowledges the data arrival. More details regarding the ACK-FBM are given in Section IV-F.

B. Buffer Information Frequency Bitmap (BI-FBM)

The BI-FBM is a frequency bitmap that collects the buffer status to be used in the buffered packet notification and inter-user interference measurement phase. The BI-FBM replaces the BI frame of LFPD-PKT. Fig. 8a shows an example of BI-FBM. Each sub-carrier is assigned to the access point and user

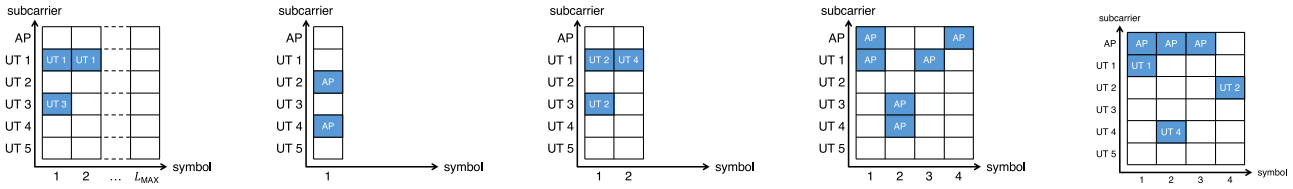

(a) BI-FBM (b) UIR-FBM (c) UII-FBM (d) SCHED-FBM (e) ACK-FBM

Fig. 8. Frequency Bitmap used in LPFD-FBM.

terminals, respectively. Each symbol represents the number of buffered packets in the access point and in each user terminal. Each node transmits the symbols of the number of buffered data packets, on the assigned sub-carrier. L_{MAX} is the maximum number of buffered packets. L_{MAX} is given a notification from the access point when the user terminal has associated to the access point. Even when a user terminal has more data packets than L_{MAX} packets, the user terminal transmits L_{MAX} symbols. In the example shown in Fig. 8a, user terminal 1 buffers two packets, and user terminal 3 has one packet for the access point.

The BI-FBM is also used for measuring inter-user interference, similarly to BI frames in LPFD-PKT. When a user terminal receives a BI-FBM containing information that some other Node-ID user terminal has buffered packets, it determines that inter-user interference occurs with the Node-ID user terminal. In contrast, when a user terminal does not receive any symbols from some Node-ID sub-carriers, it determines that inter-user interference does not occur with these user terminals.

Even if user terminal A has buffered packets and sends BI-FBM symbols, when user terminals A and B are a hidden terminal relationship pair, the inter-user interference between user terminals A and B does not occur. In that case, the BI-FBM symbol is also attenuated and does not reach the user terminal B.

C. User Interference Information Request Frequency Bitmap (UIR-FBM)

The UIR-FBM is a frequency bitmap that is used by the access point to request the inter-user interference information from the user terminals, and employed in the transmission schedule assignment phase. The UIR-FBM reduces the overhead of the UIR frames in the LPFD-PKT.

Fig. 8b shows an example of the UIR-FBM. It consists of one symbol: the sub-carrier corresponding to the user terminal, which is a downlink candidate in two-directional full-duplex communication, which is set to one by the access point. The access point selects the user terminal based on the buffered packet information gathered by the BI-FBM. In the example shown in Fig. 8b, the sub-carriers for user terminals 2 and 4 are set to one.

D. User Interference Information Frequency Bitmap (UII-FBM)

The UII-FBM is a frequency bitmap used for transmitting to the access point the inter-user interference between user terminals from each user terminal, and employed in the transmission schedule assignment phase. The UII-FBM replaces the UII frames of LPFD-PKT and reduces the overhead of UII frames.

Fig. 8c shows an example of UII-FBM. The user terminal that has been requested to send the inter-user interference information by the UIR-FBM from the access point, sends a UII-FBM. The UII-FBM from each user terminal indicates whether inter-user interference occurs between the user terminal and the two-directional full-duplex destination user terminal mentioned in the UIR-FBM. In order to reduce the UII-FBM size, each user terminal sends inter-user interference information via the following procedure: First, the user terminal receiving the UIR-FBM from the access point retrieves only the Node-ID whose assigned subcarrier is 1, and arranges the retrieved Node-ID in ascending order. Note that the retrieved Node-ID represents the user terminal, which is requested to transmit the inter-user interference information from access point in the UIR-FBM. The requested user terminals transmit the UII-FBM in accordance with the order of the retrieved Node-ID. Each user terminal sets to one the UII-FBM sub-carrier of the Node-IDs causing inter-user interference with the user terminal itself.

In the example shown in Fig. 8c, user terminals 2 and 4 send the inter-user interference information. The first symbol is assigned for user terminal 2, and the second is assigned for user terminal 4. User terminal 2 sends a symbol with the sub-carrier for Node-ID 1 and 3 set to one. Also, user terminal 4 sends a symbol with the sub-carrier for Node-ID 1 set to one.

E. Schedule Frequency Bitmap (SCHED-FBM)

The SCHED-FBM is a frequency bitmap used by the access point to notify all user terminals of the data frame transmission and reception schedule. The SCHED-FBM is used in the transmission schedule assignment phase. Fig. 8d shows an example of the SCHED-FBM. Subcarrier denotes the Node-ID of each user terminal and access point. Symbol denotes the scheduled transmission cycle. For bi-directional full-duplex communication, the access point transmits a symbol in which two subcarriers for the access point and the communication partner user terminal are set to one. In addition, for two-directional full-duplex communication, the access point transmits a symbol in which two subcarriers are set to one: one is a subcarrier for the transmitter user terminal Node-ID, the other is a

subcarrier for the receiver Node-ID. For half-duplex communication, the access point transmits a symbol where a subcarrier for a transmitter or receiver user terminal Node-ID is set to one.

In the example shown in Fig. 8d, the SCHED-FBM shows that bi-directional full-duplex communication between the access point and the user terminal 1 will be performed in the first transmission cycle; in the second transmission cycle, two-directional full-duplex communication will be performed: an uplink from user terminal 3 and a downlink to user terminal 4; in the third transmission cycle, an uplink half-duplex communication from user terminal 1 will be performed; and in the fourth transmission cycle, a downlink half-duplex communication to user terminal 2 will be performed.

Note that each user terminal can distinguish whether it is a transmitter or a receiver in two-directional full-duplex communication and half-duplex communication. This is because the bi-directional full-duplex communication has been just completed at this point, and only transmission or reception packets remain. This enables the access point to communicate the schedule of two-directional full-duplex communication and half-duplex communication by using only the UIR-FBM and SCHED-FBM.

F. Acknowledgment Frequency Bitmap (ACK-FBM)

An example of the ACK-FBM is shown in Fig. 8e. The ACK-FBM is a frequency bitmap used for acknowledgment in the data transmission and acknowledgment phase. Subcarriers represent the Node-IDs of the access point and the user terminals; symbols represent transmission cycles. When each access point and user terminal transmit received data in a given transmission cycle, the access point and user set the symbol representing the transmission cycle to 1 in the ACK-FBM. The access point and all user terminals transmit the ACK-FBMs simultaneously. In the example shown in Fig. 8e, the access point transmits ACK for the uplink transmission from user terminal 1 in the first symbol and ACK for the uplink transmission from user terminal 3 in the second symbol; user terminal 4 transmits ACK for the downlink transmission from user terminal 4 in the third symbol; and user terminal 2 transmits ACK for the downlink transmission from the user terminal 2 in the fourth symbol.

V. Analysis for Ideal Case of LPFD

In this section, we describe the analytical model of the proposed LPFD under symmetric traffic assumption that amount of uplink traffic and downlink traffic are same. We analyze the ideal case of LPFD, where arriving packets are scheduled for transmission without any overhead of control packets. We derive the expected values of the number of packets transmitted by bi-directional full-duplex, two-directional full-duplex, and half-duplex communication. First, we introduce the probability $p(\lambda, k)$ of k packet arrivals in a beacon interval t_{beacon} as $p(\lambda, k) = \exp(-\lambda t_{\text{beacon}}) \frac{(\lambda t_{\text{beacon}})^k}{k!}$, where λ is the packet arrival rate.

Then, we can obtain the expected number of packets transmitted by full-duplex ($[n_{\text{FD}}]$), and by half-duplex communication ($E[n_{\text{HD}}]$) as

$$\begin{aligned} E[n_{\text{FD}}] = 2 \sum_{k=1}^{n_{\max}-1} k \Bigg[& p(N\lambda_{\text{down}}, k) p(N\lambda_{\text{up}}, k) \\ & + p(N\lambda_{\text{down}}, k) \left\{ 1 - \sum_{j=0}^{k} p(N\lambda_{\text{up}}, j) \right\} \\ & + \left\{ 1 - \sum_{j=0}^{k} p(N\lambda_{\text{down}}, j) \right\} p(N\lambda_{\text{up}}, k) \Bigg] \\ & + 2 n_{\max} \left(1 - \sum_{k=0}^{n_{\max}-1} p(N\lambda_{\text{down}}, k) \right) \\ & \times \left(1 - \sum_{k=0}^{n_{\max}-1} p\big(N\lambda_{\text{up}}, k\big) \right), \end{aligned} \tag{4}$$

$$\begin{aligned} E[n_{\text{HD}}] = & \sum_{k=1}^{\infty} \sum_{j=0}^{\min(k, n_{\max})} \{\min(k, n_{\max}) - j\} \\ & \times \big\{ p(N\lambda_{\text{down}}, k) p(N\lambda_{\text{up}}, j) \\ & + p(N\lambda_{\text{down}}, j) p(N\lambda_{\text{up}}, k) \big\} \end{aligned} \tag{5}$$

where λ_{up} and λ_{down} represent uplink and downlink packet arrival rate for each user terminal respectively, and $n_{\max}$ is the maximum number of communication pairs (full-duplex or half-duplex) in one beacon cycle, $n_{\max} = \lfloor \frac{\text{Beacon Interval}}{\text{Data frame size / Data rate}} \rfloor (= \lfloor \frac{100\,[\text{ms}]}{1528\,[\text{byte}]/6\,[\text{Mbps}]} \rfloor = 49)$.

Then, we can obtain the expected number of packets transmitted by two-directional full-duplex communication as

$$\begin{aligned} lE[n_{\text{TFD}}] = 2 \sum_{k=1}^{n_{\max}-1} \Bigg\{ & f(k,k) p(N\lambda_{\text{down}}, k) p(N\lambda_{\text{up}}, k) \\ & + \sum_{j=k+1}^{\infty} f(k,j) p(N\lambda_{\text{down}}, k) p(N\lambda_{\text{up}}, j) \\ & + \sum_{j=k+1}^{\infty} f(k,j) p(N\lambda_{\text{down}}, j) p(N\lambda_{\text{up}}, k) \Bigg\} \\ + 2 \sum_{k=n_{\max}}^{\infty} \Bigg\{ & f(n_{\max}, k) p(N\lambda_{\text{down}}, k) p(N\lambda_{\text{up}}, k) \\ & + \sum_{j=k+1}^{\infty} f(n_{\max}, j) p(N\lambda_{\text{down}}, k) p(N\lambda_{\text{up}}, j) \\ & + \sum_{j=k+1}^{\infty} f(n_{\max}, j) p(N\lambda_{\text{down}}, j) p(N\lambda_{\text{up}}, k) \Bigg\}. \end{aligned} \tag{6}$$

where $f(k,j) = \sum_{i=0}^{k} i \binom{j}{k-i} (\frac{1}{N})^{(k-i)} (\frac{N-1}{N})^{\{i+(j-k)\}}$. The function $f(k,j)$ represents the expected number of the two-directional full-duplex transmission pairs when k full-duplex pairs are communicated (two-direction and bi-directional full-duplex), and j is the largest number of packets arrived in access point or user terminals. Combining (4) and (6), the expected

number of packets transmitted by bi-directional full-duplex communication is

$$E[n_{\mathrm{BFD}}] = E[n_{\mathrm{FD}}] - E[n_{\mathrm{TFD}}]. \quad (7)$$

Using (1)–(3) and (4)–(7), we can obtain the BPJ of ideal LPFD as

$$\mathrm{BPJ}_{\mathrm{ideal}} = \frac{\mathrm{BPJ}_{\mathrm{BFD}}E[n_{\mathrm{BFD}}] + \mathrm{BPJ}_{\mathrm{TFD}}E[n_{\mathrm{TFD}}] + \mathrm{BPJ}_{\mathrm{HD}}E[n_{\mathrm{HD}}]}{E[n_{\mathrm{BFD}}] + E[n_{\mathrm{TFD}}] + E[n_{\mathrm{HD}}]}. \quad (8)$$

Similarly to (8), power consumption and throughput can be obtained by using the expected number of packets.

VI. Performance Evaluations

We performed a computer simulation to confirm the performance of LPFD-PKT and LPFD-FBM.

A. Evaluation Environment

The star topology of the evaluation environment contains one access point and N user terminals. User terminals are placed at random positions in a 50×50 [m^2] square. The access point is placed at the center of the square. We defined a propagation model with deterministic attenuation. Each node uses a transmit power of 10 [dBm]. Carrier-sensing threshold is set to -70 [dBm]. The path loss model is defined based on [27] as follows,

$$L(d) = L_{\mathrm{FS}}(d) \quad (d \le d_{\mathrm{BP}})$$
$$L(d) = L_{\mathrm{FS}}(d_{\mathrm{BP}}) + 35\log_{10}(d/d_{\mathrm{BP}}) \quad (d > d_{\mathrm{BP}})$$

where d [m] is the distance between transmitter and receiver, d_{BP} [m] is a breakpoint distance with 5, and L_{FS} is the free space loss with slope of 2. When the interference signal is larger than the carrier-sensing threshold, the signal will interfere with the node.

Uplink traffic from each user terminal arrive according to a Poisson arrival with λ_{up} [frames/sec.]; and downlink traffic to each user terminal arrive according to a Poisson arrival with λ_{down} [frames/sec.]. When uplink and downlink arrival rates are the same, λ represents both arrival rates ($\lambda = \lambda_{\mathrm{up}} = \lambda_{\mathrm{down}}$). Frame losses occur when a frame collides with another frame. The access point and user terminals transmit data with a fixed data rate of 6 [Mbps] and data size. Beacon interval length (t_{beacon}) is 100 [ms]. We define full-duplex data loss rate ($\mathrm{Pr}_{\mathrm{fdloss}}$) to evaluate incomplete full-duplex cancellation. According to the rate $\mathrm{Pr}_{\mathrm{fdloss}}$, the packet transmitted by full-duplex communication is lost because of imperfect self-interference cancellation. The maximum number of buffered packet notifications from each user terminal and the access point is $L_{\max} = 40$ in the LPFD-FBM.

The size of each frame is defined based on the IEEE 802.11 standard [21]. Table III shows the size of each frame. The size of data frame is normally defined as 1528 [byte]; and 1528 [byte] and 68 [byte] data frames are generated in Section VI-F; The size of ACK frame is defined as 14 [byte]; The beacon frame size is defined as 28 [byte]; The size of PS-Poll frame used in IEEE 802.11 PSM is defined as 20 [byte]. In this paper, the frame sizes used in the LPFD-PKT are defined as follows: the BI frame is 28 [byte]; the UIR frame size is $20 + 6n_{\mathrm{requested}}$ [byte] when the access point requests $n_{\mathrm{requested}}$ user terminals to transmit inter-user interference information; the UII frame size is defined as $20 + 6n_{\mathrm{interference}}$ [byte] when each user terminal communicates interference with $n_{\mathrm{interference}}$ user terminals; and the SCHED frame size is $20 + 6n_{\mathrm{scheduled}}$ [byte] when the access point communicates the schedule of $n_{\mathrm{scheduled}}$ cycles data and ACK transmission. Additionally, the length of one symbol in the frequency bitmap used in the LPFD-FBM is defined as 4 [μsec.]. SIFS duration is defined as 16 [μsec.] [21].

TABLE III
Frame and Space Size

Frame and Space	Size
Data frame	1528, (68) [byte]
ACK frame	14 [byte]
Beacon frame	28 [byte]
PS-Poll frame	20 [byte]
BI frame	28 [byte]
UIR frame	$20 + 6n_{\mathrm{requested}}$ [byte]
UII frame	$20 + 6n_{\mathrm{interference}}$ [byte]
SCHED frame	$20 + 6n_{\mathrm{scheduled}}$ [byte]
One symbol of FBM in LPFD-FBM	4 [μsec.]
SIFS duration	16 [μsec.]

TABLE IV
Power Consumption of Each Circuit

Power Consumption	Value
$P_{\mathrm{CONTROL,\ ON}}$	3.00×10^2 [mW]
$P_{\mathrm{TX,\ ON}}$	5.25×10^2 [mW]
$P_{\mathrm{RX,\ ON}}$	1.95×10^2 [mW]
$P_{\mathrm{CONTROL,\ OFF}}$	49.5 [mW]
$P_{\mathrm{TX,\ OFF}}$	0.00 [mW]
$P_{\mathrm{RX,\ OFF}}$	0.00 [mW]
$P_{\mathrm{CANCEL,\ OFF}}$	0.00 [mW]
$P_{\mathrm{CANCEL,\ ON}}$	0.00–5.00×10^3 [mW]

Power consumption of each circuit is defined based on the chipset of Wi-Fi, SX-SDCAG 802.11a/b/g SDIO Card Module [28]. Table IV shows the power consumption of each circuit. $P_{\mathrm{CONTROL,\ ON}}$ is 3.00×10^2 [mW]; $P_{\mathrm{TX,\ ON}}$ is 5.25×10^2 [mW]; $P_{\mathrm{RX,\ ON}}$ is 1.95×10^2 [mW]; $P_{\mathrm{CONTROL,\ OFF}}$ is 49.5 [mW]; $P_{\mathrm{TX,\ OFF}}$ is 0.00 [mW]; $P_{\mathrm{RX,\ OFF}}$ is 0.00 [mW]; $P_{\mathrm{CANCEL,\ OFF}}$ is 0.00 [mW]. Currently, no off-the-shelf self-interference cancellation circuit for full-duplex WLAN exists. The power consumption of existing cancellation techniques, e.g., balun cancellation [1], [4], passive cancellation [3], is small enough to be neglected. In this paper, we assume a variable $P_{\mathrm{CANCEL,\ ON}}$ from 0.00 [mW] to 5.00×10^3 [mW]. The proposed algorithms and operation algorithms are implemented in a C++ based discrete event simulator with MAC/PHY parameters. Ten trials were conducted to obtain an average. In each trial, the performance value averaged over 100 seconds was acquired.

We compared the performance of the following six approaches to benchmark the LPFD-PKT and LPFD-FBM:

1) *LPFD-PKT:* LPFD-PKT is the proposed method mentioned in Section III.
2) *Low power wireless communication with half-duplexing and control packets (LPHD-PKT):* LPHD-PKT is LPFD-PKT without full-duplex communication. The difference

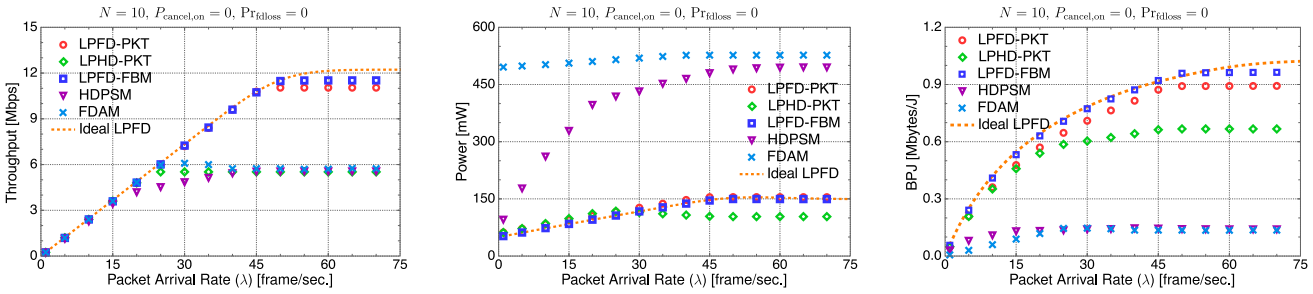

(a) Throughput (b) Power Consumption (c) Bit-per-Joule

Fig. 9. Evaluation for Increasing Packet Arrival Rate.

between LPHD-PKT and LPFD-PKT is the transmission schedule assignment. In the assignment phase of LPHD-PKT, the access point assigns the transmission only by half-duplex communication.

3) *LPFD-FBM:* LPFD-FBM is also the proposed method mentioned in Section IV. LPFD-FBM reduces the overhead of frame exchanges in LPFD-PKT by using a frequency bitmap.
4) *Full-duplex continuous active mode (FDAM):* FDAM is the normal full-duplex communication mode. MAC of FDAM is designed based on RTS/FCTS [11]. Nodes in [11] start data transmission with CSMA/CA. FDAM demonstrates a reduced energy consumption in comparison with LPFD-PKT and LPFD-FBM.
5) *Half-duplex power saving mode (HDPSM):* HDPSM is the existing half-duplex power saving mode in IEEE 802.11 [21].
6) *Ideal LPFD:* Ideal LPFD is the theoretical ideal performance of the low power full-duplex communication described in Section V. Ideal LPFD shows the performance of LPFD-PKT and LPFD-FBM when information exchange overhead does not exist. Ideal LPFD represents a theoretical limit of LPFD-PKT and LPFD-FBM.

B. Evaluation for Increasing Packet Arrival Rate

We evaluated the system performances for an increasing packet arrival rate λ. Fig. 9 shows the performance of a user terminal when the packet arrival rate changes from 1 to 70 [frames/sec.], the number of user terminals (N) is fixed at 10, power consumption of cancellation circuit ($P_{\text{CANCEL, ON}}$) is fixed at 0.0 [mW], and assuming perfect self-interference cancellation ($\Pr_{\text{fdloss}} = 0$).

Fig. 9a shows that the achieved throughput of the proposed LPFD-PKT and LPFD-FBM is close to the theoretical limit. This is because these methods efficiently scheduled the transmission based on the traffic. The throughput difference between the theoretical limit and the proposed methods is due to the overhead. LPFD-FBM achieved the higher throughput compared to LPFD-PKT, because the frequency bitmap reduces its overhead. Additionally, LPFD-PKT and LPFD-FBM achieved approximately twice the throughput of HDPSM or LPHD-PKT ($\lambda \geq 50$ [frames/sec.]). The reason is that full-duplex communication can double the transmission capacity.

Fig. 9b shows that the power consumptions of LPFD-PKT, LPHD-PKT, and LPFD-FBM are the three smallest ones, thus demonstrating the energy efficiency of the proposed scheduling methods. Power consumption of LPHD-PKT is smallest when the packet arrival rate is larger than 30 [packets/sec.] because LPHD-PKT handles approximately half the number of packets than LPFD-PKT and LPFD-PKT.

Additionally, both proposed LPFD-PKT and LPFD-FBM achieved a low power consumption near the theoretical limit (Ideal LPFD). This is because the transmission scheduling algorithm of the proposed methods efficiently manages the energy.

Fig. 9c shows that LPFD-FBM achieved the highest BPJ, and LPFD-PKT is the second highest. LPFD-FBM achieved approximately 4.1 times the BPJ of HDPSM ($\lambda = 15$ [frames/sec.]) and up to approximately 6.9 times the BPJ of HDPSM ($\lambda = 70$ [frames/sec.]), approximately 6.0 times the BPJ of FDAM ($\lambda = 15$ [frames/sec.]), and approximately 7.1 times the BPJ of FDAM ($\lambda = 1$ [frames/sec.]). Additionally, BPJ of both proposed LPFD-PKT and LPFD-FBM approached the theoretical limit for an increasing packet arrival rate. This is because the control packet transmission is dominant in comparison with the data frame transmission when the packet arrival rate is low, thus decreasing the BPJ. The LPFD-FBM achieved a higher BPJ if compared to LPFD-PKT, because the frequency bitmap reduces the control frame overhead. On the other hand, the BPJ of HDPSM decreases for an increasing packet arrival rate, because in this method each user terminal gains the transmission and reception rights by a contention mechanism that constantly forces the user terminal in awake state until the end of the transmission is reached in the beacon interval.

C. Evaluation for Increasing Number of User Terminals

In Section VI-B, the performance evaluation with a fixed number of user terminals is reported. In this section, we evaluate the performance with a variable number of user terminals, with a constant packet arrival rate (λ) is fixed at 15 [frames/sec.]; the power consumption of cancellation circuit ($P_{\text{CANCEL, ON}}$) is fixed at 0.0 [mW], and assuming perfect self-interference cancellation ($\Pr_{\text{fdloss}} = 0$).

First, we comment the results of the throughput evaluation. Fig. 10a shows the throughput when the number of user terminals (N) changes from 2 to 45. It can be seen that the

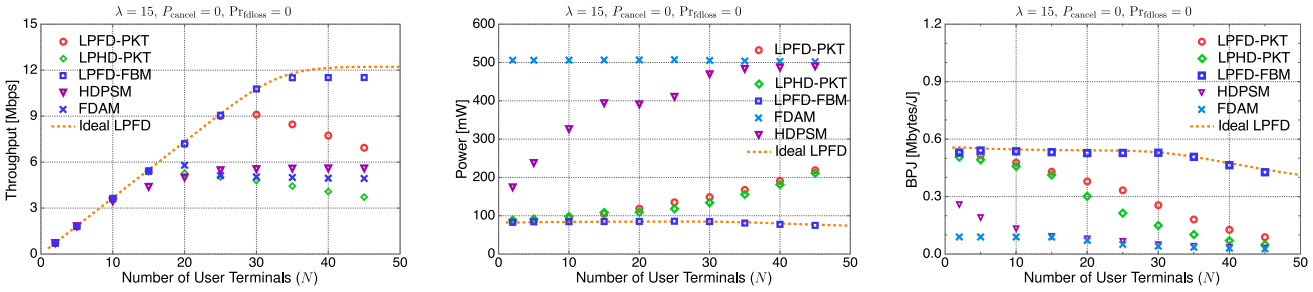

(a) Throughput (b) Power Consumption (c) Bit-per-Joule

Fig. 10. Evaluation for Increasing Number of User Terminals.

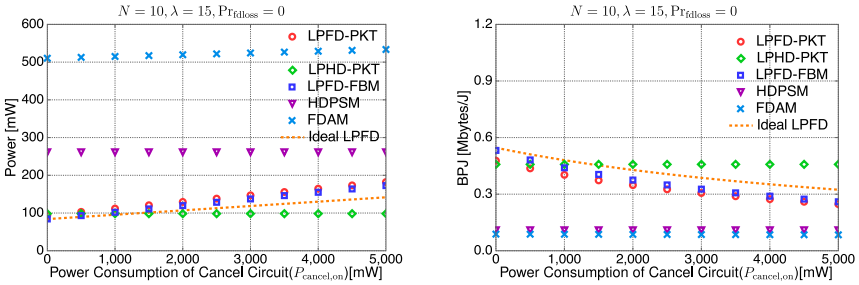

(a) Power Consumption (b) Bit-per-Joule

Fig. 11. Evaluation for Increasing Cancellation Circuit Power Consumption.

throughput of proposed LPFD-PKT and LPFD-FBM perform close to the theoretical limit. This is due to their efficient transmission scheduling based on traffic. The LPFD-FBM achieved the highest throughput because the frequency bitmap reduces the LPFD-PKT overhead. The throughput of LPFD-PKT decreases with an increasing number of user terminal when the number of user terminals is larger than 30 ($N \geq 30$); the throughput of LPHD-PKT decreases when the number of user terminals becomes larger than 15 ($N \geq 15$). The overhead of information exchange by packets increases with the number of user terminals, and suppress the data transmission. Additionally, LPFD-FBM achieved approximately twice the throughput of the HDPSM when the number of user terminals is larger than 35 ($N \geq 35$). This is because full-duplex communication doubles the capacity.

Second, we analyze the power consumption results. Fig. 10b shows the power consumption of a user terminal when the number of user terminals changes from 2 to 45. The power consumption of the LPFD-FBM is the lowest. Both proposed LPFD-PKT and LPFD-FBM maintain their low power consumption with an increasing number of user terminals. The power consumption of LPFD-PKT and LPFD-FBM are less than approximately one-fifth of the FDAM. In contrast, the power consumption of the HDPSM increased with the number of user terminals. This is because the contention mechanism used in HDPSM increases the overhead with the number of competitors (user terminals).

Finally, we illustrate the BPJ evaluation. Fig. 10c shows the BPJ when the number of user terminals changes from 2 to 45. LPFD-FBM achieved the highest BPJ, approximately 2.1 times higher than that of LPFD-PKT, and approximately 10.1 times higher than that of the HDPSM when the number of user terminals is 30. This is because the frequency bitmap used in the LPFD-FBM reduces the overhead of exchanging LPFD-PKT buffer information. When the number of user terminals is large, the reduction of overhead owing to the frequency bitmap effect is higher.

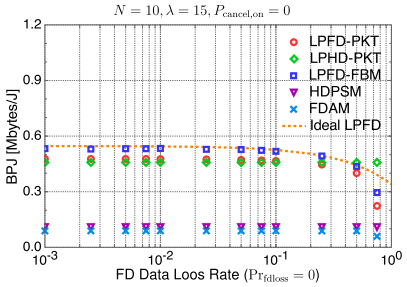

Fig. 12. Bit-per-Joule vs. Full-duplex Cancellation Performance.

D. Evaluation for Increasing Cancellation Circuit Power Consumption

There is no off-the-shelf self-interference cancellation circuit for full-duplex communication. Power consumption of the self-interference cancellation circuits is expected to be very low. From Sections VI-B to VI-C, the performance is evaluated for a power consumption of the cancellation circuit ($P_{\text{CANCEL, ON}}$) is fixed at 0.0 [mW]. However, it is expected that the energy efficiency (BPJ) of the proposed method decreases with the increase of the cancellation circuit power consumption. We evaluated the power consumption of a user terminal

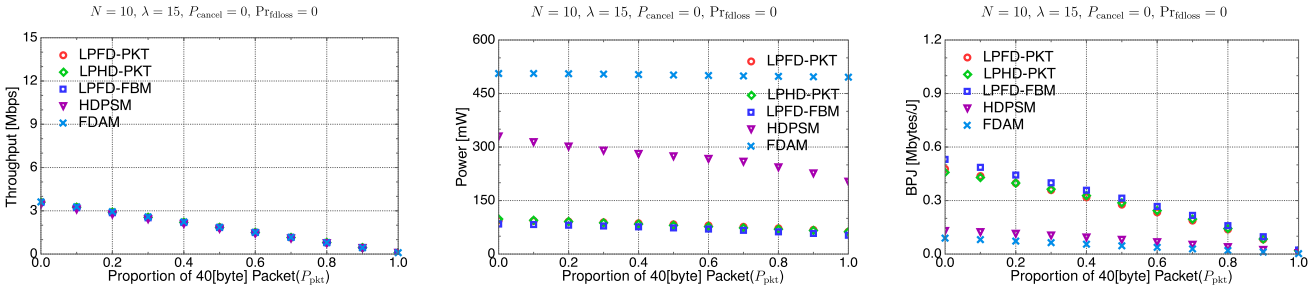

(a) Throughput (b) Power Consumption (c) Bit-per-Joule

Fig. 13. Evaluation for Variable Packet Length.

and its BPJ when the power consumption of the interference cancellation changes from 0.00 [mW] to 5.00×10^3 [mW], with a number of user terminals (N) is fixed at 10, a packet arrival rate (λ) is fixed at 15 [frames/sec.], and assuming perfect self-interference cancellation ($\Pr_{\text{fdloss}} = 0$).

First, we illustrate the evaluation of power consumption. Fig. 11a shows the power consumption of a user terminal when the power consumption of interference cancellation changes from 0.00 [mW] to 5.00×10^3 [mW]. The power consumption of LPFD-PKT, LPFD-FBM, and FDAM increase linearly with the increasing power consumption of the cancel circuit. When the power consumption of the cancellation circuit is less than 5.00×10^3 [mW], the proposed LPFD-PKT and LPFD-FBM have a power consumption lower than HDPSM.

Additionally, we evaluate the BPJ. Fig. 11b shows the BPJ when the power consumption of the interference cancellation changes from 0.00 [mW] to 5.00×10^3 [mW]. The results show the same trend as for power consumption: the BPJ of the proposed LPFD-PKT and LPFD-FBM is larger than HDPSM.

E. Evaluation for Imperfect Full-Duplex Cancellation

From Sections VI-B to VI-D, we assumed perfect full-duplex cancellation. In this section, we assume a situation where full-duplex performance drops due to imperfect full-duplex cancellation.

Fig. 12 shows the BPJ performance when full-duplex data loss rate ($\Pr_{\text{fdloss}}$) changes from 1.0×10^{-3} to 0.75×10^0, with a number of user terminal (N) is fixed at 10, a packet arrival rate (λ) is fixed at 15 [frames/sec.], a power consumption of cancellation circuit ($P_{\text{cancel, on}}$) is fixed at 0.0 [mW]. The LPFD-FBM achieves the highest BPJ when the full-duplex data loss rate is in the range 1.0×10^{-3} to 0.25×10^0. The BPJ of the proposed LPFD-PKT and LPFD-FBM decrease with an increasing full-duplex data loss rate. However, the proposed LPFD-PKT and LPFD-FBM achieve a higher BPJ, compared to HDPSM, even when full-duplex data loss rate ($\Pr_{\text{fdloss}}$) is 0.5×10^0.

F. Evaluation for Variable Packet Length

We performed an evaluation under variable packet size scenario. Variable packet size is derived from practical packet size distribution described in [29]. The actual packets size without header seems mostly bimodal at 40 [byte] and 1500 [byte] [29]. We evaluated the performance by changing a proportion of 68 [byte] packets and 1528 [byte] packets with MAC header.

Fig. 13 shows the performances when the traffic proportion of 68 [byte] size packets changes from 0 to 1.0, with a number of user terminal (N) is fixed at 10, a packet arrival rate (λ) is fixed at 15 [frames/sec.], a power consumption of cancellation circuit ($P_{\text{cancel, on}}$) is fixed at 0.0 [mW], and assuming perfect self-interference cancellation ($\Pr_{\text{fdloss}} = 0$). Fig. 13a shows that the throughput of all methods is the same whatever the proportion of 68 [byte] packets. Fig. 13b shows that the proposed LPFD-PKT and LPFD-FBM have a reduced power consumption. Fig. 13c shows that the difference in BPJ decreases when the proportion of 68 [byte] packets increases. Under practical traffic environment, where the proportion of 68 [byte] packet is around 40 % according to [29], the BPJ performance of the proposed methods is high.

G. Evaluation Under Asymmetric Uplink and Downlink Traffic

We conducted the performance evaluation with a variable ratio of uplink and downlink traffic keeping a fixed total amount of traffic. Fig. 14 shows the performance with a variable uplink packet arrival rate (λ_{up}) from 3.0 [frames/sec.] to 75.0 [frames/sec.], with a number of user terminals (N) is fixed at 10, a downlink packet arrival rate (λ_{down}) is fixed at 15 [frames/sec.], a power consumption of cancellation circuit ($P_{\text{cancel, on}}$) is fixed at 0.0 [mW], and assuming perfect self-interference cancellation ($\Pr_{\text{fdloss}} = 0$).

Fig. 14a shows that the proposed LPFD-PKT and LPFD-FBM achieved the highest throughput. The power consumption of LPFD-FBM, as shown in Fig. 14b, is the lowest. Fig. 14c shows that the BPJ of proposed LPFD-PKT and LPFD-FBM is high regardless of the ratio of uplink and downlink traffic. Even if the uplink arrival rate decreases, the power consumption of the HDPSM does not decrease because HDPSM attempts to reduce only the power consumption of downlink. In contrast to the HDPSM, the proposed method try to reduce both power consumptions of uplink and downlink.

H. Power Consumption of Single User Terminal

In this section, we evaluated the power consumption of a single user terminal. Fig. 15 shows the power consumption, when the packet arrival rate (λ) is 15, the number of user

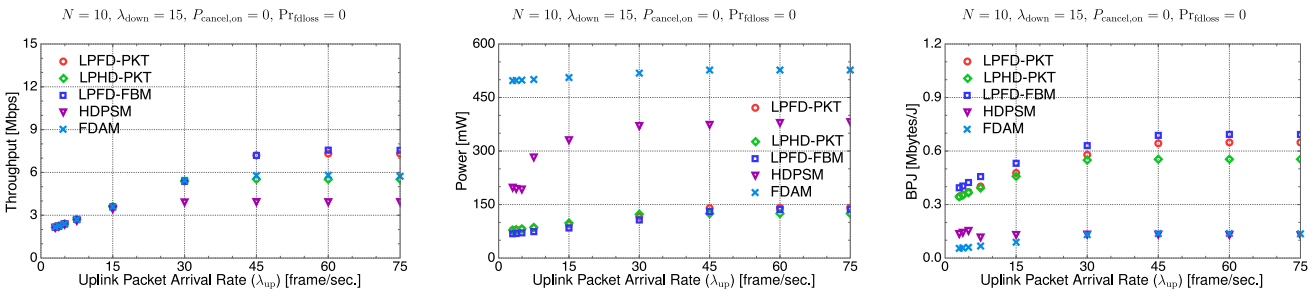

(a) Throughput (b) Power Consumption (c) Bit-per-Joule

Fig. 14. Evaluation on Asymmetric Uplink and Downlink Traffic.

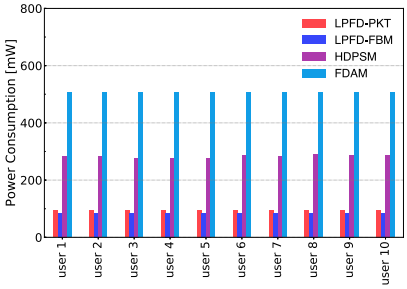

Fig. 15. Power Consumption of Each User Terminal.

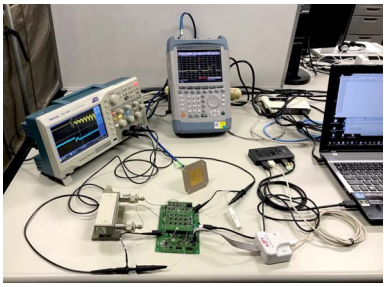

Fig. 16. Experimental Setup.

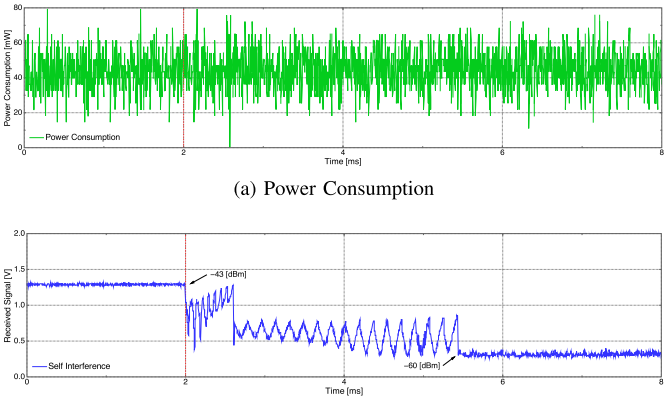

(a) Power Consumption

(b) Received Signal

Fig. 17. Experimental Evaluation of Active Cancellation Circuit.

terminals (N) is fixed at 10, power consumption of cancellation circuit ($P_{\text{CANCEL, ON}}$) is fixed at 0.0 [mW], and perfect self-interference cancellation occurs ($\text{Pr}_{\text{fdloss}} = 0$). Although user terminals are randomly placed in space, the power consumption of each user terminal is almost the same, and there is no bias. Fig. 15 shows that the proposed LPFD-PKT and LPFD-FBM reduce the power consumption by approximately 400 [mW] with respect to the overall power consumption of full-duplex communication (FDAM). The proposed methods reduced the power consumption to approximately one-fifth of FDAM and one-third of HDPSM for all user terminals in the network.

VII. Discussion

To show that under some condition power consumption of cancellation is very small, we implemented both active and passive analog cancellation. Fig. 16 shows the experimental setup. For power consumption measurements, we used a Texas Instruments CC2531 as a transmitter and measured the performance and power consumption of cancellation circuit with a Tektronix TBS 1202B oscilloscope.

Fig. 17 shows the power consumption and cancellation performance of an active cancellation circuit, employing device QHx220 as in [2] and [4]. In Fig. 17a, horizontal axis is time, and vertical axis is power consumption. We turned on the active cancellation circuit at 2 [ms]. The dashed line represents a moving average of energy consumption per 0.2 [ms]. In Fig. 17b, horizontal axis is time, and vertical axis is the received signal of self-interference. When the power is turned on, the active cancellation circuit starts the calibration. In the example shown in Fig. 17b, the calibration was completed 3.5 [ms] after turning on the power. As shown in Fig. 17a, the active cancellation circuit consumes approximately 40 [mW] and its performance was approximately 17 [dB] as shown in Fig. 17b.

Fig. 18 shows the power consumption and cancellation performance of a passive cancellation circuit. The dashed line represents the moving average of energy consumption per 0.2 [ms]. The passive cancellation circuit comprises phase shifters and an attenuator array as described in [1]. We turned on the passive cancellation circuit at 2 [ms], and the calibration was completed in 3.3 [ms]. As shown in Fig. 18a, the power consumption of passive cancellation is approximately 50 [mW] during the calibration, and approximately 25 [mW] after the calibration, thus lower than the power consumption of QHx220 active cancellation.

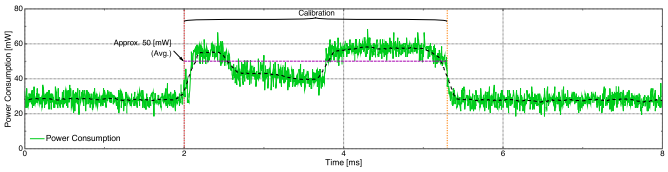

(a) Power Consumption

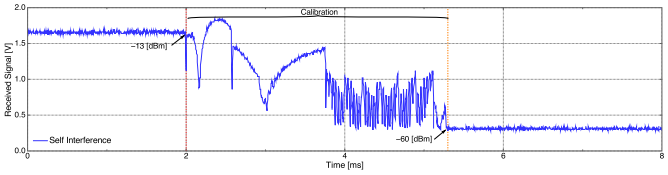

(b) Received Signal

Fig. 18. Experimental Evaluation of Passive Cancellation Circuit.

Active cancellation circuit consumes a lot of energy because active cancellation requires oscillators operation. Theoretically, the energy consumption of passive cancellation circuit is nearly zero, because they operate passively the received signal. Our experiments show that the passive cancellation circuit consumes 25 [mW] since the implemented circuits are made of commercial off-the-shelf parts, comprising 4 phase shifters, 4 attenuators, and decoder circuits for controlling the phase shifters and attenuators. These components contain redundant circuits to be used for various purposes, since these general-purpose products are not optimized for the self-interference cancellation. For example, attenuators have a function capable of handling both serial and parallel interfaces. By designing an LSI chip optimized for these applications, the power consumption could be reduced to a much lower level.

VIII. Conclusion

In this paper, we proposed LPFD-PKT and LPFD-FBM to reduce energy consumption and enhance energy efficiency (Bit-per-Joule) of user terminals in wireless networks. Both LPFD-PKT and LPFD-FBM enhance energy efficiency by scheduling bi-directional full-duplex communication, two-directional full-duplex communication, and half-duplex communication. Additionally, LPFD-FBM reduces the overhead of exchanging buffered packet information in LPFD-PKT by using a frequency bitmap. Performance evaluation shows that both LPFD-PKT and LPFD-FBM achieve higher energy efficiency compared to the IEEE 802.11 PSM and existing full-duplex MAC protocol.

References

[1] D. Bharadia, E. McMilin, and S. Katti, "Full duplex radios," in *Proc. Annu. Conf. ACM Special Interest Group Data Commun. (ACM SIGCOMM)*, Hong Kong, Aug. 2013, pp. 375–386.

[2] J. I. Choi, M. Jain, K. Srinivasan, P. Levis, and S. Katti, "Achieving single channel, full duplex wireless communication," in *Proc. 16th ACM Annu. Int. Conf. Mobile Comput. Netw. (ACM MobiCom)*, Chicago, IL, USA, Sep. 2010, pp. 1–12.

[3] E. Everett, A. Sahai, and A. Sabharwal, "Passive self-interference suppression for full-duplex infrastructure nodes," *IEEE Trans. Wireless Commun.*, vol. 13, no. 2, pp. 680–694, Feb. 2014.

[4] M. Jain *et al.*, "Practical, real-time, full duplex wireless," in *Proc. 17th ACM Annu. Int. Conf. Mobile Comput. Netw. (ACM MobiCom)*, Las Vegas, NV, USA, Sep. 2011, pp. 301–312.

[5] J. Bai and A. Sabharwal, "Distributed full-duplex via wireless side-channels: Bounds and protocols," *IEEE Trans. Wireless Commun.*, vol. 12, no. 8, pp. 4162–4173, Aug. 2013.

[6] D. Kim, H. Lee, and D. Hong, "A survey of in-band full-duplex transmission: From the perspective of PHY and MAC layers," *IEEE Commun. Surveys Tuts.*, vol. 17, no. 4, pp. 2017–2046, 4th Quart., 2015.

[7] M. Duarte *et al.*, "Design and characterization of a full-duplex multiantenna system for WiFi networks," *IEEE Trans. Veh. Technol.*, vol. 63, no. 3, pp. 1160–1177, Mar. 2014.

[8] W. Choi, H. Lim, and A. Sabharwal, "Power-controlled medium access control protocol for full-duplex WiFi networks," *IEEE Trans. Wireless Commun.*, vol. 14, no. 7, pp. 3601–3613, Jul. 2015.

[9] A. Tang and X. Wang, "Medium access control for a wireless LAN with a full duplex AP and half duplex stations," in *Proc. IEEE Glob. Commun. Conf. (IEEE GLOBECOM)*, Austin, TX, USA, Feb. 2014, pp. 4732–4737.

[10] A. Tang and X. Wang, "A-duplex: Medium access control for efficient coexistence between full-duplex and half-duplex communications," *IEEE Trans. Wireless Commun.*, vol. 14, no. 10, pp. 5871–5885, Oct. 2015.

[11] W. Cheng, X. Zhang, and H. Zhang, "RTS/FCTS mechanism based full-duplex MAC protocol for wireless networks," in *Proc. IEEE Globecom Workshops (IEEE GC Wkshps)*, Atlanta, GA, USA, Dec. 2013, pp. 5017–5022.

[12] S. Sen, R. R. Choudhury, and S. Nelakuditi, "CSMA/CN: Carrier sense multiple access with collision notification," in *Proc. 16th Annu. Int. Conf. Mobile Comput. Netw. (ACM MobiCom)*, Chicago, IL, USA, Sep. 2010, pp. 25–36.

[13] Y. Zhang, L. Lazos, K. Chen, B. Hu, and S. Shivaramaiah, "FD-MMAC: Combating multi-channel hidden and exposed terminals using a single transceiver," in *Proc. 33rd Annu. IEEE Int. Conf. Comput. Commun. (IEEE INFOCOM)*, Toronto, ON, Canada, Apr. 2014, pp. 2742–2750.

[14] D. Nguyen, L.-N. Tran, P. Pirinen, and M. Latva-Aho, "On the spectral efficiency of full-duplex small cell wireless systems," *IEEE Trans. Wireless Commun.*, vol. 13, no. 9, pp. 4896–4910, Sep. 2014.

[15] S. Y. Chen, T.-F. Huang, K. C.-J. Lin, H.-W. P. Hong, and A. Sabharwal, "Probabilistic medium access control for full-duplex networks with half-duplex clients," *IEEE Trans. Wireless Commun.*, vol. 16, no. 4, pp. 2627–2640, Apr. 2017.

[16] K. Tamaki *et al.*, "Full duplex media access control for wireless multi-hop networks," in *Proc. IEEE 77th Veh. Technol. Conf. (IEEE VTC Spring)*, Dresden, Germany, Jun. 2013, pp. 1–5.

[17] T. Vermeulen and S. Pollin, "Energy-delay analysis of full duplex wireless communication for sensor networks," in *Proc. IEEE Glob. Commun. Conf. (IEEE GLOBECOM)*, Austin, TX, USA, Dec. 2014, pp. 455–460.

[18] X. Xie and X. Zhang, "Does full-duplex double the capacity of wireless networks?" in *Proc. 33rd Annu. IEEE Int. Conf. Comput. Commun. (IEEE INFOCOM)*, Toronto, ON, Canada, Apr. 2014, pp. 253–261.

[19] T. Riihonen, S. Werner, and R. Wichman, "Hybrid full-duplex/half-duplex relaying with transmit power adaptation," *IEEE Trans. Wireless Commun.*, vol. 10, no. 9, pp. 3074–3085, Sep. 2011.

[20] R. Murakami, M. Kobayashi, S. Saruwatari, and T. Watanabe, "An energy efficient MAC for wireless full duplex networks," in *Proc. IEEE Globecom Workshops (IEEE GC Wkshps)*, Washington, DC, USA, Dec. 2016, pp. 1–6.

[21] *IEEE Standard for Information Technology–Telecommunications and Information Exchange Between Systems Local and Metropolitan Area Networks–Specific Requirements Part 11: Wireless LAN Medium Access Control (MAC) and Physical Layer (PHY) Specifications*, IEEE Standard 802.11-2012, Mar. 2012.

[22] S. Sen, R. R. Choudhury, and S. Nelakuditi, "No time to countdown: Migrating backoff to the frequency domain," in *Proc. 17th Annu. Int. Conf. Mobile Comput. Netw. (ACM MobiCom)*, Las Vegas, NV, USA, Sep. 2011, pp. 241–252.

[23] X. Feng, J. Zhang, Q. Zhang, and B. Li "Use your frequency wisely: Explore frequency domain for channel contention and ACK," in *Proc. 31st IEEE Conf. Inf. Commun. (IEEE INFOCOM)*, Orlando, FL, USA, Mar. 2012, pp. 549–557.

[24] J. Fang *et al.*, "Fine-grained channel access in wireless LAN," *IEEE/ACM Trans. Netw.*, vol. 21, no. 3, pp. 772–787, Jun. 2013.

[25] A. Dutta, D. Saha, D. Grunwald, and D. Sicker, "SMACK: A SMart ACKnowledgment scheme for broadcast messages in wireless networks," in *Proc. Annu. Conf. ACM Special Interest Group Data Commun. (ACM SIGCOMM)*, Barcelona, Spain, Aug. 2009, pp. 15–26.

[26] D. Halperin, J. Ammer, T. Anderson, and D. Wetherall, "Interference cancellation: Better receivers for a new wireless MAC," in *Proc. 6th Workshop Hot Topics Netw. (HotNets-VI)*, College Park, MD, USA, Nov. 2007, pp. 1–6.
[27] V. Erceg *et al.*, *TGn Channel Models*, IEEE Standard 802.11-03/940r4, pp. 1–45, May 2004.
[28] *802.11 a/b/g SDIO Card Module Ultracompact Wireless Solution for Embedded Applications*, Silex Technol., Midvale, UT, USA, 2010. [Online]. Available: http://www.mouser.com/ds/2/367/sx-sdcag_brief-2825.pdf
[29] R. Sinha, C. Papadopoulos, and J. Heidemann, "Internet packet size distributions: Some observations," USC/Inf. Sci. Inst., Marina Del Rey, CA, USA, Tech. Rep. ISI-TR-2007-643, May 2007.

Makoto Kobayashi (S'15) received the M.E. degree from Osaka University, Japan, in 2016. He is currently pursuing the Ph.D. degree with the Graduate School of Information Science and Technology, Osaka University, Japan, and has been a Research Fellow (DC2) of the Japan Society for the Promotion of Science, since 2017. His research interests include wireless networks and communications, especially MAC protocol to support diversified requirements and services. He is a student member of IEEE ComSoc, IPSJ, and IEICE.

Ryo Murakami received the B.E. degree from Osaka University, Osaka, Japan, in 2016, where he is currently pursuing the M.S. degree with the Department of Information Networking, Graduate School of Information Science and Technology. His research interests include medium access control protocol in wireless networks, with a focus on power consumption reduction.

Kazuhiro Kizaki is a Project Research Associate with the Graduate School of Information Science and Technology, Osaka University, Japan. He joined Communication Equipment Works, Mitsubishi Electric Corporation, in 1970. He specializes in RF circuits and antennas.

Shunsuke Saruwatari received the B.E. degree from the University of Electro-Communications, Japan, in 2002, and the M.S. and Ph.D. degrees from the University of Tokyo, Japan, in 2004 and 2007, respectively. He is an Associate Professor with the Graduate School of Information Science and Technology, Osaka University, Japan. In 2007, he was a Visiting Researcher with the Illinois Genetic Algorithms Laboratory, University of Illinois at Urbana-Champaign. From 2008 to 2011, he was a Research Associate with the Research Center for Advanced Science and Technology, University of Tokyo, Japan. From 2012 to 2015, he was a tenure-track Assistant Professor with the Graduate School of Informatics, Shizuoka University, Japan. His research interests are in the areas of wireless networks, sensor networks, and system software. He is a member of ACM, IPSJ, and IEICE.

Takashi Watanabe (S'83–M'87) received the B.E., M.E., and Ph.D. degrees from Osaka University, Japan, in 1982, 1984, and 1987, respectively. He has been a Professor with the Graduate School of Information Science and Technology, Osaka University, Japan, since 2013. He joined the Faculty of Engineering, Tokushima University in 1987 and moved to the Faculty of Engineering, Shizuoka University in 1990. He was a Visiting Researcher with the University of California, Irvine, CA, USA, from 1995 to 1996. He has served on many program committees for networking conferences, IEEE, ACM, IPSJ, IEICE. His research interests include mobile networking, ad hoc sensor networks, IoT/M2M networks, intelligent transport systems, specially MAC and routing. He is a member of IPSJ and IEICE.